

ARPES evidence for a Quasiparticle Liquid in overdoped $\text{Bi}_2\text{Sr}_2\text{CaCu}_2\text{O}_{8+\delta}$ B.O. Wells⁺, Z. Yusof*Department of Physics, University of Connecticut
Storrs, CT 06269, USA*

T. Valla, A.V. Fedorov, P. Johnson

*Department of Physics, Brookhaven National Laboratory
Upton, NY 11973, USA*

C. Kendziora

*Naval Research Laboratory
Washington, DC 20375, USA*

S. Jian, D. Hinks

*Materials Sciences Division, Argonne National Laboratory
Argonne, IL 60439, USA*

Received (to be inserted)

Revised by publisher)

High resolution angle-resolved photoemission spectroscopy of highly overdoped $\text{Bi}_2\text{Sr}_2\text{CaCu}_2\text{O}_{8+\delta}$ with a $T_c = 51\text{K}$ indicates that the basic transport processes in this material are fundamentally different from both the lesser doped cuprates as well as model metallic compounds. The overdoped sample has sharp ARPES peaks at the Fermi energy throughout the Brillouin zone even in the normal state, unlike the lesser-doped compounds. In particular, the spectra near $(\pi,0)$ point show the presence of a sharp peak well above T_c . The ARPES lineshapes, and thus the self energy, at a given energy are almost independent of k . Further, the quasiparticle scattering rate at the Fermi energy seems to be closely tied to direct resistivity measurements. This leads us to the conclusion that overdoped $\text{Bi}_2\text{Sr}_2\text{CaCu}_2\text{O}_{8+\delta}$ is best described as a quasiparticle liquid. However, the energy dependence of the scattering rates is quite similar to that found in the lesser-doped compounds and quite different from that seen in a typical metal.

A central question in research on highly correlated electron materials is under what conditions, if ever, are such materials well described by the Fermi Liquid¹ model. This has been particularly true for the normal state of the cuprate, high- T_c superconductors. For the optimally doped, and certainly the underdoped cuprates, there are many results that indicate that the Fermi Liquid picture may not be valid^{2,3} in the normal state. It is speculated that as doping increases beyond the optimal value, the cuprate may become a Fermi Liquid.⁴ However, there is little experimental evidence from the highly overdoped regime showing Fermi Liquid properties. Moreover, recently the term Fermi Liquid has been used in the literature to describe a variety of different properties and behaviors of metals making the term imprecise. In the strictest definition of a Fermi Liquid, transport properties are governed by quasiparticles whose self-energy, Σ , is proportional to the square of binding energy, $\square\omega$, and temperature, T , reflecting the electron-electron interactions. For regular metals, this is not the case for most T and ω because the electron-phonon interaction dominates the scattering rate and the resistivity. At the other extreme, the term Fermi Liquid has been used to describe any material that has well defined single-particle excitations, regardless of the details of the scattering rates or whether transport proceeds via these quasiparticles. In

order to be precise and avoid the ambiguities in the literature, we coin the term “quasiparticle liquid” as a way to describe a system that has: (i) well-defined single-particle excitations around the Fermi surface, and (ii) transport properties which are dominated by the quasiparticles even if they do not have the classic ω^2 and T^2 behavior or the electron-phonon behavior of typical metals.

Here we focus on the overdoped $\text{Bi}_2\text{Sr}_2\text{CaCu}_2\text{O}_{8+\delta}$, the material expected to be most Fermi Liquid like. Comparison to the lesser-doped cuprates allows us to understand how the electronic structure evolves with doping. Similarly, comparison to the dispersion and structure of the Mo(110) surface state demonstrates properties that remain unlike that seen in typical metals. We conclude that the overdoped cuprate is best described as quasiparticle liquid because well-defined single particle excitations are present around the entire Fermi surface and they appear to govern transport. Nonetheless, important properties of the spectral function are similar to the lesser-doped cuprates and markedly different from a standard metal surface state. These include the linear dependence of $\text{Im}\Sigma$ on energy and the insensitivity of the scattering rate to temperature changes across T_c . Thus we explicitly describe the challenge to theory in

constructing the temperature and doping dependence of Σ .

Angle-resolved photoemission spectroscopy (ARPES) is, in principle, the best method to determine the nature of the quasiparticles in two-dimensional solids. The presence of a sharp peak in the spectra indicates the presence of a long-lived single particle excitation, or quasiparticle. The presence of such a sharp peak has been used to argue for the presence of a Fermi Liquid below T_c in under and optimally doped cuprates, though clearly DC transport does not proceed through such a single particle channel.⁵ The normal state of the optimally doped samples does have a sharp peak at the Fermi energy, but at specific k values, the nodal direction. In the superconducting state, a well-defined sharp peak appears around the Fermi surface but only for a very limited range of ω and is unrelated to transport. In fact, for most ω and k values, the spectral function blows up into a broad, ill-defined excitation. Over the energy and k range where a peak can be defined, Σ is unlike that for a typical metal.² In model 2D metals, the extracted Σ values are amenable to analyses in terms of traditional scattering mechanisms.⁶ More exotic phenomenologies have been invoked to understand similar data for the optimally doped cuprate.²

Single crystals of $\text{Bi}_2\text{Sr}_2\text{CaCu}_2\text{O}_{8+\delta}$ were synthesized using the floating-zone technique⁷ that yielded optimal T_c onset of 95 K. Overdoping was achieved by annealing the samples in oxygen at 400 C for 5 days, yielding $T_c \sim 51$ K.⁸ The samples were kept in the cells under oxygen pressure until they were mounted in the vacuum chamber. The crystals were cleaved in situ at T below 150 K under vacuum with a base pressure of 8×10^{-11} Torr. Crystal orientation was determined using low-energy electron diffraction (LEED). All data shown here were obtained within 12 hours after cleaving to minimize variation in doping content of the exposed surface with time. T_c of the samples were determined to be $\sim 51 \pm 5$ K using a SQUID magnetometer. All ARPES measurements were performed at beamline U13UB at the NSLS with photon energy of 22 eV and a Scienta SES 200 hemispherical analyzer that simultaneously collects a large energy (0.5 to 1 eV) and angular (12°) window. This allows for the simultaneous collection of the photoemission intensity as a function of binding energy (energy distribution curve or EDC) and momentum (momentum distribution curve or MDC) along a particular direction in the BZ.² The resulting energy resolution is ~ 10 meV with an angular resolution of better than 0.2° .

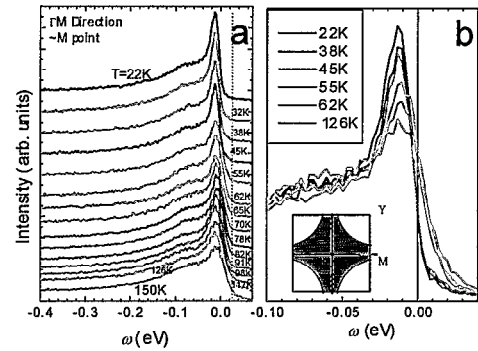


Fig. 1 EDCs for OD Bi2212 ($T_c = 51$ K) near the M-point (see inset) at various temperatures. The data in Fig. 1(a) have been shifted vertically for clarity. Six representative spectra are shown unshifted in Fig. 1(b).

Fig. 1(a) shows the T dependence of the EDC's near the M-point (ΓM direction) of the Brillouin zone. The spectra show a well-defined sharp peak along with a broader hump. The overall shape persists well into the normal state, a behavior that was also seen in a similar overdoped sample by another group.⁹ This is noticeably different than the optimal- and under-doped cuprates where the sharp peak disappears around T_c .¹⁰ A recent report¹¹ shows the sharp peak disappearing at slightly above T_c on lightly overdoped crystals and claims the peak intensity is a measure of the superfluid density. This cannot be the case for our more overdoped samples since the sharp peak persists to temperatures well above T_c where there is no superfluid.⁹ The only change in lineshape as T goes above T_c is a shift in the leading edge to signify the closing of the gap, as shown in Fig 1(b). The gap size estimated from this shift is 10 meV, which is consistent with that observed in tunneling measurements on similar crystals.¹²

A visual demonstration of the different energy ranges over which the ARPES excitation is well defined shown in Fig. 2 for the $\text{Bi}_2\text{Sr}_2\text{CaCu}_2\text{O}_{8+\delta}$ cuprates as well as for Mo(110). When compared to the lower-doped cuprates, the ARPES spectrum of the overdoped sample shows a larger range of ω and k over which the spectral peak is well defined. k_F for the overdoped sample in this direction is measured to be 0.39 \AA^{-1} or $0.34(\pi, \pi)$, compared to 0.446 \AA^{-1} or $0.391(\pi, \pi)$ for optimally doped $\text{Bi}_2\text{Sr}_2\text{CaCu}_2\text{O}_{8+\delta}$,² indicating a shift of the Fermi surface towards the Γ point. In contrast to these samples, the Mo shows well-defined peaks over the entire band. Clearly the ω range over which the ARPES spectra is well defined is much greater for the overdoped sample versus either the under or optimally doped samples, but still less than that for the Mo.

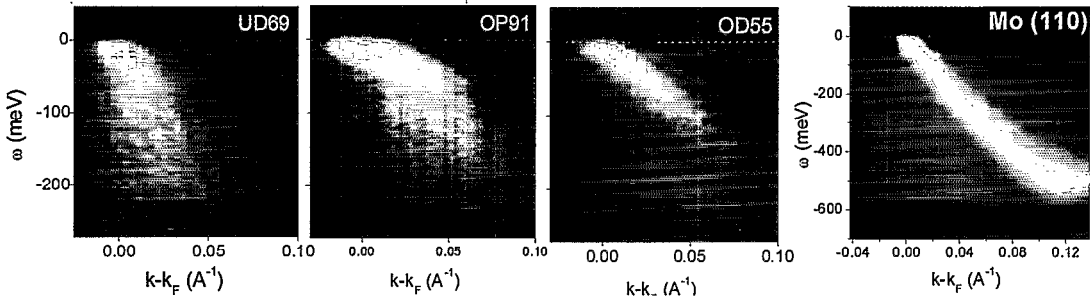


Fig. 2. Photoemission intensity as a function of ω and k for three different cuprates doping levels and the Mo(110) surface state. The spectra for the cuprates are along the gap node direction, or Γ -M.

The width Δk of the MDC spectra in the Γ Y region is used to obtain $\text{Im}\Sigma$ using the relation $\hbar v_k \Delta k \sim 2\text{Im}\Sigma$,² where v_k is the non-interacting band velocity.¹³ Fig. 3 shows $\text{Im}\Sigma$ at $T = 22$ K along with similar data for both optimally doped $\text{Bi}_2\text{Sr}_2\text{CaCu}_2\text{O}_{8+\delta}$ and the Mo surface state. We note that within the error bars, $\text{Im}\Sigma$ for the overdoped sample above T_c shows similar behavior to that shown in the figure. None of the data sets in the figure show $\text{Im}\Sigma$ varying as ω^2 for small energies. As noted previously, the Mo data can be broken into contributions from three scattering mechanisms: electron-electron, electron-phonon, and defect scattering.⁶ The phonon mechanism dominates in the vicinity of E_F . Unlike Mo, $2\text{Im}\Sigma$ for the over- and the optimally doped $\text{Bi}_2\text{Sr}_2\text{CaCu}_2\text{O}_{8+\delta}$ ² have a predominantly linear dependence on ω . For the optimally doped sample, the slope of $\text{Im}\Sigma$ versus ω is much greater and follows a characteristic Marginal Fermi Liquid (MFL) behavior where $\text{Im}\Sigma \sim \max(\omega, T)$.¹⁴ Such an identification is less clear in the overdoped sample, but appears possible. Certainly the overdoped sample does not seem to be easily analyzed in terms of the typical scattering processes in metals. Overall, the peak broadening that gives $\text{Im}\Sigma$ for the overdoped sample lies in-between the behavior of the optimally doped cuprate and the Mo.

In both the normal and superconducting state, Σ of the overdoped cuprate is much less k dependent than for the lesser-doped compounds. This is made clear by examining the ARPES lineshape for a band position at a given energy but different k values, i.e. different parts of the Brillouin zone. Fig. 4(a) and (b) compare the overdoped EDC's from the two in-plane symmetry directions at several binding energies, both below and above T_c . There is a remarkable similarity in the lineshape along Γ M and Γ Y. The main difference is that the remnant broad hump seen for $\omega_p \sim 12$ meV is only present in the Γ M spectra. This hump becomes less pronounced at higher ω where the spectra look more similar to each other. We compare this to

optimally doped $\text{Bi}_2\text{Sr}_2\text{CaCu}_2\text{O}_{8+\delta}$ (Fig. 4c) where there is a dramatic difference between the spectra from the two directions. This is especially true above T_c where there is no well-defined peak in the Γ M spectrum. The difference in lineshapes is even stronger in underdoped $\text{Bi}_2\text{Sr}_2\text{CaCu}_2\text{O}_{8+\delta}$. We conclude that well-defined ARPES peaks occur over a much greater k range in the normal state of the overdoped compound versus the optimally or under-doped material.¹⁵ In particular Σ seems to be k independent in the overdoped material. It could be argued that with increasing hole doping, the influence of the antiferromagnetic “environment” in the system becomes weaker. This is consistent with the weaker coupling strength with increasing doping observed in the nodal direction.¹³

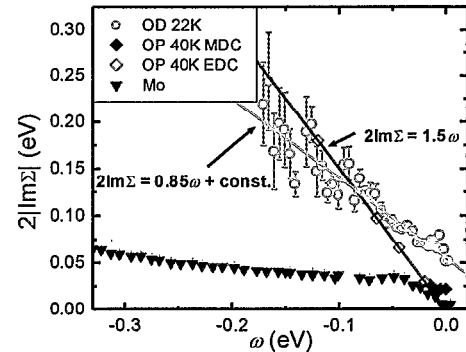


Fig. 3. $2\text{Im}\Sigma$ in the Γ Y direction for the overdoped cuprate, the optimally doped cuprate ($T_c = 91$ K),² and Mo(110) surface state.⁶ The values shown in the legend are the temperatures where the ARPES spectra were obtained. $2\text{Im}\Sigma$ for the overdoped was obtained exclusively from the MDC spectra, whereas the values for the optimally doped sample were obtained from both MDC and EDC. The scattering due to impurities has been subtracted from the Mo data. The straight lines are guides to the eye.

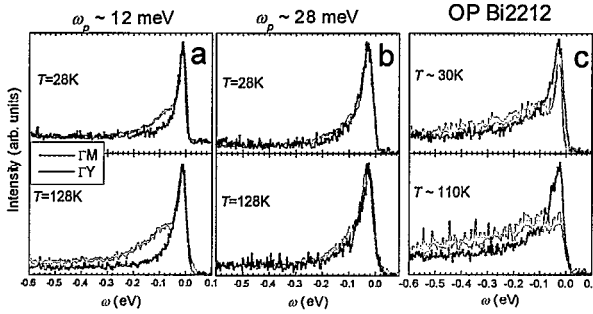


Fig. 4. EDC lineshapes for the over-doped (a and b) and optimally doped (c) $\text{Bi}_2\text{Sr}_2\text{Ca}\text{Cu}_2\text{O}_{8+\delta}$ taken at the M-point and the nodal direction. Each data set has been normalized to the intensity of the sharp peak, except the normal state of the optimally doped cuprate where it has not been normalized. ω_p is the binding energy of the peak intensity.

In conventional metals, transport is governed by quasiparticles that scatter due to interactions with other excitations. The resistivity, ρ , in these materials is related to the lifetime or the mean free path via Boltzmann transport theory that involves an integral over the Fermi surface.¹⁶ Although the lifetimes of ARPES quasiparticles are not identical to that in transport measurements, they should be governed and should be the same for temperatures well above absolute zero. For the overdoped samples, we have quasiparticles that are well defined over the whole Fermi surface and scattering rates that are largely k -independent as seen in Fig. 4. Thus, it is realistic to consider that in this case, the Boltzmann transport formulation would produce a meaningful comparison between the lifetime and the in-plane resistivity ρ_{ab} .

The Boltzman result appropriate for this case is $\rho = (2\pi\hbar/e^2S)\lambda^{-1}$, with S the area of the Fermi surface in reciprocal space and λ the mean free path. The ARPES data give both S and λ . S is found by considering the Fermi surface a cylinder of radius 0.75\AA^{-1} centered at the X or Y points of the Brillouin zone. λ is given by $1/\Delta k$, the inverse width of the MDC at the Fermi energy, and appears to be almost constant around the Fermi surface. Thus ρ_{ab} is directly proportional to Δk . Note that this relationship only provides a numerical value for the temperature dependent term. Typically in resistivity measurements there are differing constant offsets due to different amounts of impurities. Such a constant offset is particularly likely here because the ARPES technique will probe defects in the surface region that may be quite different than the bulk.

Figure 5 shows a comparison of the ARPES Δk data with ρ_{ab} .⁸ The resistivity data comes from a different crystal that is overdoped to have the same T_c , the best comparison available. As outlined above, the ARPES linewidth is scaled as $A\Delta k + B$ for comparison to the resistivity. The constant offset between the two data sets is negative, but does not appear to have any simple meaning. The linear term is smaller by a factor of 1/6 than the value expected from the calculation above. It is not clear at this time if such a discrepancy indicates a serious problem with the model as applied to the cuprate or is the best that can be expected given the uncertainties involved. Nevertheless, ρ_{ab} and Δk have the same functional form in the normal state. If the ARPES quasiparticles were not dominant in transport there is no reason to expect any correspondence between the two quantities. A clear example of the latter situation is the superconducting state. The evolution of the quasiparticle Δk is smooth through T_c while ρ_{ab} drops abruptly to zero because transport proceeds through a two-particle channel not directly measured in ARPES. The smooth variation of Δk through T_c is also seen along the nodal direction in optimally doped $\text{Bi}_2\text{Sr}_2\text{Ca}\text{Cu}_2\text{O}_{8+\delta}$.¹⁵

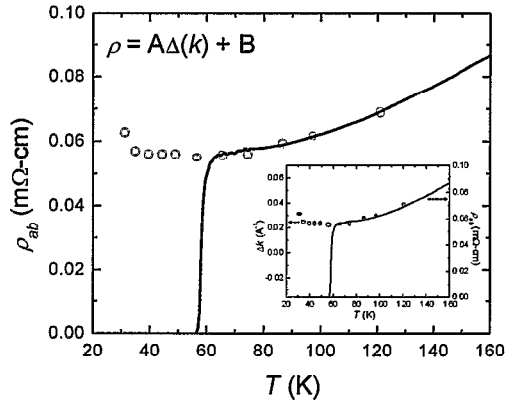


Fig. 5. A comparison of the ARPES Δk (open circles) and experimental ρ_{ab} (solid line) from OD Bi2212 with $T_c = 58\text{K}$.⁸

Other recent ARPES studies of overdoped $\text{Bi}_2\text{Sr}_2\text{Ca}\text{Cu}_2\text{O}_{8+\delta}$ have indicated the presence of two non-degenerate bands arising out of interaction of the CuO bilayers.^{17,18} While our data (not shown) may indicate evidence for a two-component Fermi surface, the specific labeling of the hump feature in the EDC spectra near $(\pi, 0)$ as the bonding band¹⁷ is inconsistent with our data due to the temperature dependence and trends of relative peak intensities with doping as shown in Fig 1. The idea of interplane coupling appearing in the overdoped samples may be understood in terms of the results reported here. The inter-plane coupling is

dominated by states near the M-points of the Brillouin zone.¹⁹ These results show the presence of more well defined quasiparticles in those regions for the overdoped samples. Thus one expects increased interplane coupling and thus splitting of the CuO plane bands due to the bilayer. Furthermore, the well-defined quasiparticle near the M points would promote coherent transport in the *c* direction. This has been shown to be the case as the *c*-axis resistivity decreases and becomes metallic with increasing doping.²⁰

The combined data indicate a somewhat subtle conclusion. The overdoped $\text{Bi}_2\text{Sr}_2\text{CaCu}_2\text{O}_{8+\delta}$ is best understood as a quasiparticle liquid in the normal state. Nonetheless, it is certainly not a Fermi Liquid in the strict sense and also does not have quasiparticle lifetimes similar to our model metal, the Mo surface state. The key elements of the ARPES data in the overdoped sample that lead to a quasiparticle description are: (i) the presence of well-defined peaks in the ARPES spectra over a wide range of T , ω and k , along with well defined peaks for the entire Fermi surface, (ii) Σ that is largely k independent, and (iii) ρ_{ab} that is proportional to the inverse mean free path measured in ARPES as expected from simple Boltzman transport. On the other hand, all of the $\text{Bi}_2\text{Sr}_2\text{CaCu}_2\text{O}_{8+\delta}$ cuprates have an $\text{Im}\Sigma$ that appears to be linear in ω . In addition, in all of the cuprates the temperature variation of Δk is insensitive to T_c . The former seems to indicate that the fundamental interactions between the electrons and other excitations are similar for all of the cuprates, and not like those for a typical metal. It remains unclear whether a true phase transition has taken place between the normal states of variously doped cuprates. The presence of well-defined excitations in the normal state seems to begin near the nodal direction and spread in energy and k with increased doping, making it difficult to define an order parameter that distinguishes between the states. Clarifying this point will be a focus of future work.

Work supported in part by Dept. of Energy under contract number DE-AC02-98CH10886, DE-FG02-00ER45801, and DOE-BES W-31-109-ENG-38. BW would like to thank the A.P. Sloan Foundation for partial support through a Research Fellowship.

References

1. P. Nozieres, *Theory of Interacting Fermi Systems* (Addison-Wesley, Reading, 1964).
2. T. Valla *et al.*, *Science* **285**, 2110 (1999).
3. P.W. Anderson, *Theory of Superconductivity in the High- T_c Cuprates* (Princeton University Press, Princeton NJ, 1997).
4. B. Batlogg and C.M. Varma, *Phys. World* **13**, 2 (2000).
5. A. Kaminski *et al.*, *Phys. Rev. Lett.* **84**, 1788 (2000).
6. T. Valla *et al.*, *Phys. Rev. Lett.* **83**, 2085 (1999).
7. N. Miyakawa *et al.*, *Phys. Rev. Lett.* **80**, 157 (1998).
8. C. Kendziora *et al.*, *Physica C* **257**, 74 (1996).
9. S. Rast *et al.*, *Europhys. Lett.* **51**, 103 (2000).
10. A.V. Fedorov *et al.*, *Phys. Rev. Lett.* **82**, 2179 (1999).
11. D.L. Feng *et al.*, *Science* **289**, 277 (2000).
12. J.F. Zasadzinski *et al.*, *cond-mat/0102475*.
13. P.D. Johnson *et al.*, *cond-mat/0102260*.
14. C.M. Varma *et al.*, *Phys. Rev. Lett.* **63**, 1996 (1989).
15. T. Valla *et al.*, *Phys. Rev. Lett.* **85**, 828 (2000).
16. N.W. Ashcroft and N.D. Mermin, *Solid State Physics* (Saunders, 1976).
17. D.L. Feng *et al.*, *Phys. Rev. Lett.* **86**, 5550 (2001).
18. Y.-D. Chuang *et al.*, *cond-mat/0102386*.
19. L.B. Ioffe and A.J. Millis, *Science* **285**, 1241 (1999); A.I. Liechtenstein *et al.*, *Phys. Rev. B* **54** (1996).
20. Y.F. Yan *et al.*, *Phys. Rev. B* **52**, 751 (1995); T. Watanebe *et al.*, *Phys. Rev. Lett.* **79**, 2113 (1997).